

Preparation, friction and wear properties of hydrophobic lanthanum borate nanorods in rapeseed oil

Ke-cheng GU¹, Bo-shui CHEN¹, Xue-mei WANG², Jiu WANG¹,
Jian-hua FANG¹, Jiang WU¹, Li-chuan HUANG³

1. Department of Oil Application and Management Engineering, Logistical Engineering University, Chongqing 401311, China;

2. Department of Chemistry and Materials Engineering, Logistical Engineering University, Chongqing, 401311, China;

3. Ministry of Supplies and Oil, Chengdu Military Region, Chengdu 610015, China

Received 21 October 2013; accepted 14 January 2014

Abstract: Oleic acid (denoted as OA) surface-capped lanthanum borate nanorods, abbreviated as OA/LaBO₃·H₂O, were prepared via hydrothermal method. The microstructures of the as-prepared OA/LaBO₃·H₂O nanorods were characterized by X-ray diffraction (XRD) and scanning electron microscopy (SEM) techniques. The friction and wear properties of OA/LaBO₃·H₂O nanorods in rapeseed oil were evaluated with a four-ball tribo-tester. The results show that the as-prepared OA/LaBO₃·H₂O nanorods are hydrophobic and display nanorods morphology with uniform diameter of about 50 nm and length of up to 500 nm. In the meantime, OA/LaBO₃·H₂O nanorods can obviously improve the anti-wear and friction-reducing capacities of rapeseed oil, and the optimal anti-wear and friction-reducing properties of rapeseed oil were obtained at an OA/LaBO₃·H₂O content of 1% (mass fraction).

Key words: lanthanum borate; nanorod; hydrophobicity; preparation; friction; wear; rapeseed oil

1 Introduction

During the last decades, much attention has been paid to nanoscale materials with fascinating physical and chemical properties [1–4]. In the field of tribology, intensive studies have been conducted to pursue a variety of inorganic nanomaterials as lubricant additives, such as metal [5,6], oxide [7–9], sulfide [10,11], fluoride [12–14] and borate nanoparticles [15,16]. Among various inorganic nanoparticles as lubricant additives, lanthanum borate nanoparticles are of special significance owing to their excellent tribological properties [17–20]. Unfortunately, the application of lanthanum borate nanoparticles in tribology is restrained owing to their poor oil solubility. The key issue in enhancing the compatibility between additives and base oil is the surface modification method using organic compounds [21,22].

The properties of nanomaterials are highly dependent on the composition, size, shape, crystal structure and surface properties [23]. One-dimensional

(1D) nanomaterials possess strikingly different chemical and physical properties due to the low dimensions of nanometer-size magnitude, which differ greatly from those of their bulk counterparts [24,25]. The previous studies on the tribological properties of lanthanum borate mainly included those of amorphous or three-dimensional nanoparticles [18–20], and no report is currently available about the preparation and tribological properties of lanthanum borate nanorods. If lanthanum borates are fabricated in the form of 1D nanorods, they will help us to understand the tribological properties of lanthanum borate nanorods and to further study the relationship between the tribological performance and the structure of lubrication additives. Herein, lanthanum borate nanorods modified by oleic acid were prepared and their friction and wear properties in rapeseed oil (abbreviated as RP) were investigated.

2 Experimental

2.1 Materials

Oleic acid (OA) was chemical grade, and the other

reagents used in the experiments were of analytical grade and were employed without further purification. Distilled water was applied for all preparation and treatment processes.

2.2 Preparation of hydrophobic lanthanum borate nanorods

2.86 g $\text{Na}_2\text{B}_4\text{O}_7 \cdot 10\text{H}_2\text{O}$ was dissolved into 50 mL distilled water under vigorously stirring for 1 h. Resultant solution was marked as A. 2.15 g $\text{La}(\text{NO}_3)_3 \cdot 6\text{H}_2\text{O}$ was dissolved into 50 mL anhydrous ethanol, followed by the addition of 2% OA (mass fraction), and the resultant mixture was marked as B. The obtained B was added dropwise into A while being stirred for 1 h at ambient temperature. After addition, the pH value of the mixture was adjusted to 13 with diluted sodium hydroxide solution. The resultant mixture was kept on stirring for 1 h and then transferred into a 200 mL Teflon-lined stainless-steel autoclave filled with anhydrous ethanol up to 80% of the total volume, sealed and maintained at 180 °C for 8 h. The final mixture was then filtered, washed repeatedly with distilled water and anhydrous ethanol to remove the unreacted reactants, OA and by-products, followed by drying at 80 °C for 4 h in air to obtain the final white lanthanum borate powders.

The non-modified lanthanum borate ($\text{LaBO}_3 \cdot \text{H}_2\text{O}$) was prepared in the same manner while no OA was added in B.

2.3 Characterization of hydrophobic lanthanum borate nanorods

The crystalline structure of the as-prepared products was analyzed with an X-ray diffractometer (XRD, Rigaku Dmax-2500, Cu K_α radiation). The thermal stability of the as-prepared products was evaluated with a thermal analyzer (Hitatch DR/4000). Infrared (IR) spectra were measured on an infrared spectrometer (Perkin-Elmer 400). The morphology and size of the as-prepared products were determined by a field emission scanning electron microscope (SEM, S-4800, JEOL), while the element compositions of samples were analyzed with an energy dispersive X-ray spectrometer (EDS) attached to the SEM. The chemical species on the worn surfaces of steel balls were analyzed with an X-ray photoelectron spectroscopy (XPS, Thermo ESCALab-250, exciting source: Al radiation; reference: contaminated carbon (C 1s: 284.80 eV)). Water contact angles of the products were measured on a contact angle goniometer (Easydrop DSA14). The sample was first pressed into a wafer with an IR powder-pressed machine under 15 MPa pressure for 2 min. The dispersing stability of lubrication oil was measured with a TG16-WS high speed centrifuge. 1 g sample was set into 10 mL of RP, resultant dispersion was heated at 348 K for 2 h in an ultrasonic bath and

then transferred into a centrifuge tube, and centrifuged at 10000 r/min for 5 min. The precipitate was dried in a desiccator and then weighted to the nearest 0.1 mg, at last the percentage of precipitate was obtained [26].

2.4 Friction and wear tests

The as-prepared OA/ $\text{LaBO}_3 \cdot \text{H}_2\text{O}$ and $\text{LaBO}_3 \cdot \text{H}_2\text{O}$ nanorods were separately dispersed ultrasonically into rapeseed oil. The wear scar diameters (WSD) and friction coefficients were measured with an MMW-1P universal four-ball friction and wear tester at 392 N and 1200 r/min for 60 min. GCr15 bearing steel balls with a diameter of 12.7 mm and a hardness of HRC 59–61 were adopted to assemble the frictional pair. Prior to tests, the balls and specimen holders were cleaned in an ultrasonic bath with petroleum ether for 10 min and then dried with a hair dryer.

3 Results and discussion

3.1 Characterization of as-prepared OA/ $\text{LaBO}_3 \cdot \text{H}_2\text{O}$ and $\text{LaBO}_3 \cdot \text{H}_2\text{O}$ nanorods

Figure 1 shows the XRD pattern of the as-prepared products. It can be observed from Fig. 1 that all diffraction peaks can be indexed as an orthorhombic structure with the lattice parameters of $a=0.5872$ nm, $b=0.8257$ nm and $c=0.5107$ nm, which are in good agreement with the standard diffraction (JCPDS files No. 12-0762). The shape of diffraction peaks indicates that the products should be well crystallized. No characteristic peaks of impurities, such as $\text{La}(\text{NO}_3)_3$, other borate and other unreacted compounds were detected, indicating that the products with high purity were obtained.

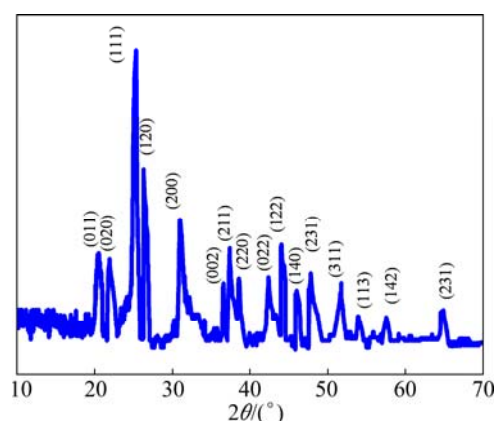


Fig. 1 XRD pattern of OA/ $\text{LaBO}_3 \cdot \text{H}_2\text{O}$ nanorods

EDS spectrum of the OA/ $\text{LaBO}_3 \cdot \text{H}_2\text{O}$ nanorods is shown in Fig. 2. It can be seen that the sample is composed of elements La, B and O (H cannot be identified). Moreover, quantitative analysis from EDS gives that the molar ratio of La to B to O is 1:1.02:4.05, which is very close to the stoichiometry of $\text{LaBO}_3 \cdot \text{H}_2\text{O}$.

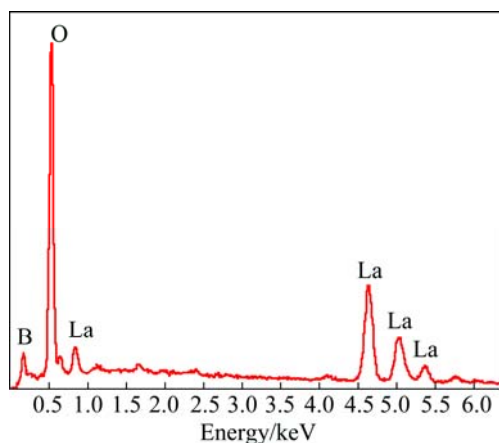


Fig. 2 EDS profile of OA/LaBO₃·H₂O

SEM images of LaBO₃·H₂O and OA/LaBO₃·H₂O are shown in Fig. 3. According to Fig. 3(a), the LaBO₃·H₂O nanorods are irregular with diameters in the range of 50–70 nm and lengths in the range of 100–250 nm; while in Fig. 3(b), the OA/LaBO₃·H₂O nanorods have a uniform diameter with an average of about 50 nm and a length of up to 500 nm, which indicates that OA plays an important role in the preparation of lanthanum borate nanorods and can obviously improve the aspect ratio of LaBO₃·H₂O nanorods.

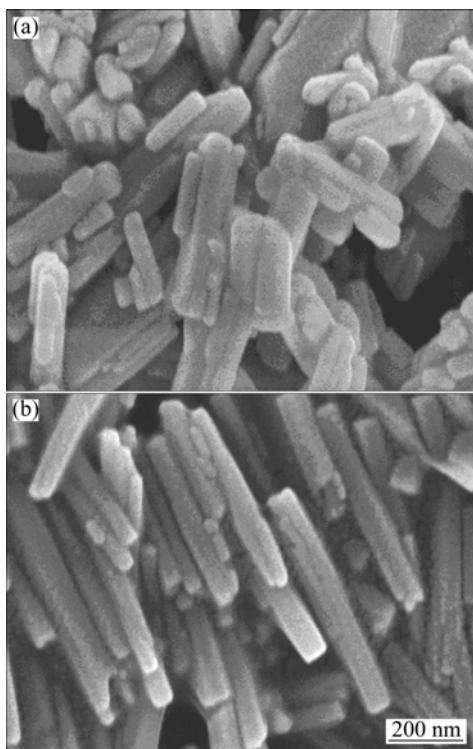


Fig. 3 SEM images of LaBO₃·H₂O (a) and OA/LaBO₃·H₂O (b)

The IR spectra of neat OA, LaBO₃·H₂O and OA/LaBO₃·H₂O are shown in Fig. 4. According to Figs. 4(a) and (b), the bands at 3458 and 3362 cm⁻¹ are

attributed to the O—H stretch vibrations, and the band at 1636 cm⁻¹ is ascribed to the bending vibration of H—O—H, which indicates that lanthanum borate nanorods contain crystal water. The bands at 1380 and 944 cm⁻¹ are assigned to the asymmetric and symmetric stretching of B(3)—O, respectively. The bands at 755 cm⁻¹ and below 670 cm⁻¹ are ascribed to the B(3)—O out-of-plane and in-plane bending vibrations [27], respectively. This result confirms the presence of the BO₃ groups and shows that the main component of the product is LaBO₃·H₂O, which is in agreement with the EDS analysis. It can be seen from Figs. 4(b) and (c) that the bands at 2927 and 2856 cm⁻¹ are attributed to the asymmetric and symmetric stretch vibrations of —CH₂—, respectively. The intensive peak at 1712 cm⁻¹ is attributed to carbonyl stretch vibration of OA. This peak, however, disappears in the IR spectrum of OA/LaBO₃·H₂O. Meanwhile, the bands at around 1142 and 1032 cm⁻¹ are attributed to carbonyl stretch vibrations of carboxylate, which indicates that chemical reaction has taken place between OA and O—H on the surface of LaBO₃·H₂O with a hydrogen bond [28].

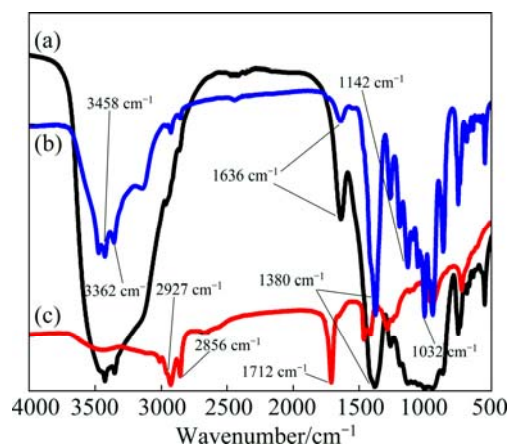


Fig. 4 IR spectra of LaBO₃·H₂O (a), OA/LaBO₃·H₂O (b) and pure OA (c)

The TGA curves of LaBO₃·H₂O and OA/LaBO₃·H₂O nanorods are shown in Fig. 5. It can be observed from Fig. 5(a) that the mass loss of LaBO₃·H₂O is 8.42% from 100 to 440 °C, which is due to the loss of one molar equivalent of the crystal water. The OA/LaBO₃·H₂O sample, into which 2.0% of OA is added, has a total mass loss of 10.23% from 100 to 440 °C. Mass loss increases quickly from 150 to 420 °C, because of the decomposition of the organic group of OA and the crystal water of sample [28]. The amount of OA calculated by TGA is about 2%, which is equal to that added in the preparation process.

In order to investigate the surface characteristics, the water contact angles of the samples were measured (Fig. 6). The water contact angle of LaBO₃·H₂O is

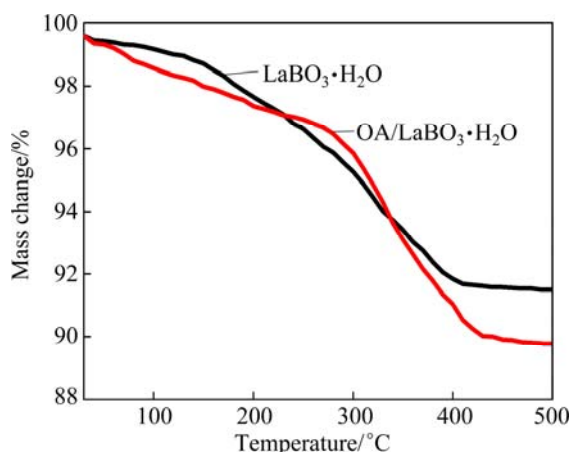


Fig. 5 TGA curves of $\text{LaBO}_3 \cdot \text{H}_2\text{O}$ and $\text{OA/LaBO}_3 \cdot \text{H}_2\text{O}$

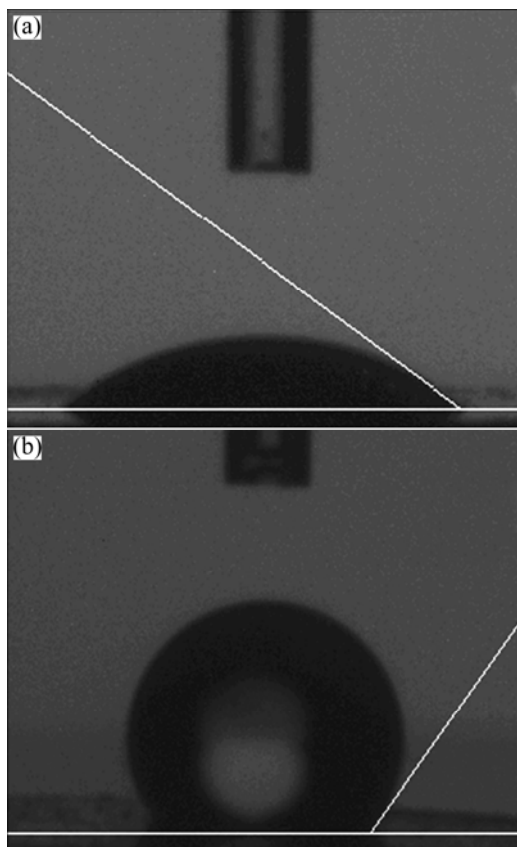


Fig. 6 Water contact angles of $\text{LaBO}_3 \cdot \text{H}_2\text{O}$ (a) and $\text{OA/LaBO}_3 \cdot \text{H}_2\text{O}$ (b)

40.11° , which indicates that $\text{LaBO}_3 \cdot \text{H}_2\text{O}$ is hydrophilic. When the samples are modified with OA, the water contact angle increases from 40.11° to 125.44° . This demonstrates that the surface of $\text{OA/LaBO}_3 \cdot \text{H}_2\text{O}$ exhibits hydrophobicity, which is in good agreement with the IR analysis.

To investigate the dispersing stability of $\text{LaBO}_3 \cdot \text{H}_2\text{O}$ and $\text{OA/LaBO}_3 \cdot \text{H}_2\text{O}$ in RP, the mass fraction of precipitates was tested (Fig. 7). It can be seen from Fig. 7 that the mass fraction of $\text{LaBO}_3 \cdot \text{H}_2\text{O}$ is 99% and

that of $\text{OA/LaBO}_3 \cdot \text{H}_2\text{O}$ is 1.2%, which indicates that the dispersing stability of $\text{OA/LaBO}_3 \cdot \text{H}_2\text{O}$ in RP is much better than that of $\text{LaBO}_3 \cdot \text{H}_2\text{O}$ in RP. The reason for the excellent dispersing stability of $\text{OA/LaBO}_3 \cdot \text{H}_2\text{O}$ in RP may be attributed to the effect of surface modification of OA.

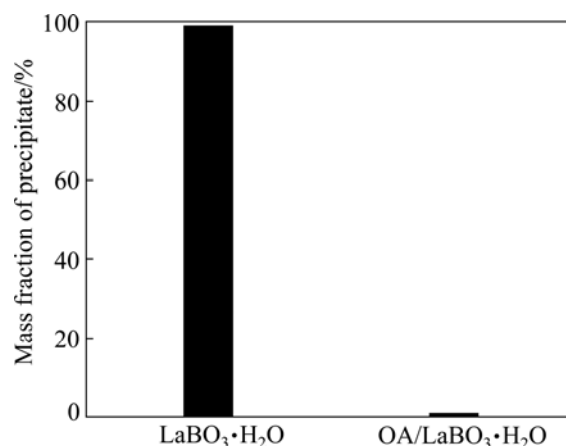


Fig. 7 Mass fractions of $\text{LaBO}_3 \cdot \text{H}_2\text{O}$ and $\text{OA/LaBO}_3 \cdot \text{H}_2\text{O}$ in RP

3.2 Friction and wear properties of $\text{OA/LaBO}_3 \cdot \text{H}_2\text{O}$ nanorods as additives in rapeseed oil

The friction coefficients of GCr15 steel balls lubricated with RP containing 1% of different additives are shown in Fig. 8. It can be observed that RP containing $\text{OA/LaBO}_3 \cdot \text{H}_2\text{O}$ provides much lower friction coefficients than RP. This indicates that $\text{OA/LaBO}_3 \cdot \text{H}_2\text{O}$ nanorods can obviously improve the friction-reducing ability of RP. However, RP containing $\text{LaBO}_3 \cdot \text{H}_2\text{O}$ provides higher friction coefficients than RP. This might be attributed to the poor solubility of $\text{LaBO}_3 \cdot \text{H}_2\text{O}$ in RP.

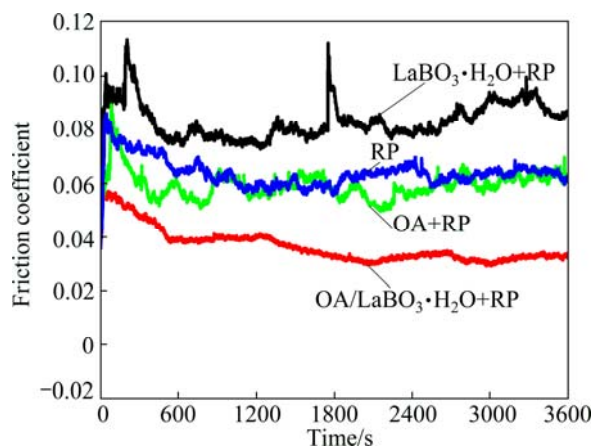


Fig. 8 Friction coefficients of GCr15 steel balls lubricated with different lubrication oils

Figure 9 shows the friction coefficients and WSD of GCr15 steel balls lubricated by RP containing different contents of $\text{OA/LaBO}_3 \cdot \text{H}_2\text{O}$ nanorods. It can be seen that

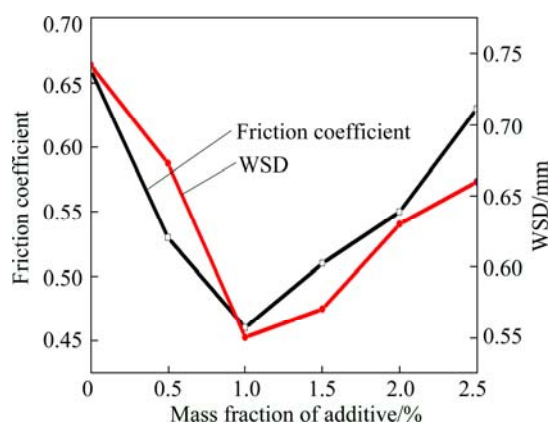


Fig. 9 Friction coefficients and WSD of GCr15 steel balls lubricated by RP with different contents of OA/LaBO₃·H₂O

the friction coefficient and WSD decrease at first as the content of OA/LaBO₃·H₂O increases up to a point, and then begin to increase as the content of OA/LaBO₃·H₂O in RP increases. The optimal friction-reducing and anti-wear capacities of RP are obtained at an OA/LaBO₃·H₂O content of 1% (mass fraction). However, elevating the content of OA/LaBO₃·H₂O above 1% leads to the decrease in friction-reducing and anti-wear capacities of RP, which might be attributed to the agglomeration of OA/LaBO₃·H₂O nanorods under frictional heat [29].

Figure 10 shows the XPS spectra of C 1s, Fe 2p, La 3d, B 1s and O 1s on the worn steel surface lubricated with RP+OA/LaBO₃·H₂O. The C 1s peak at 288.5 eV reveals the existence of carbonyl groups (Fig. 10(a)),

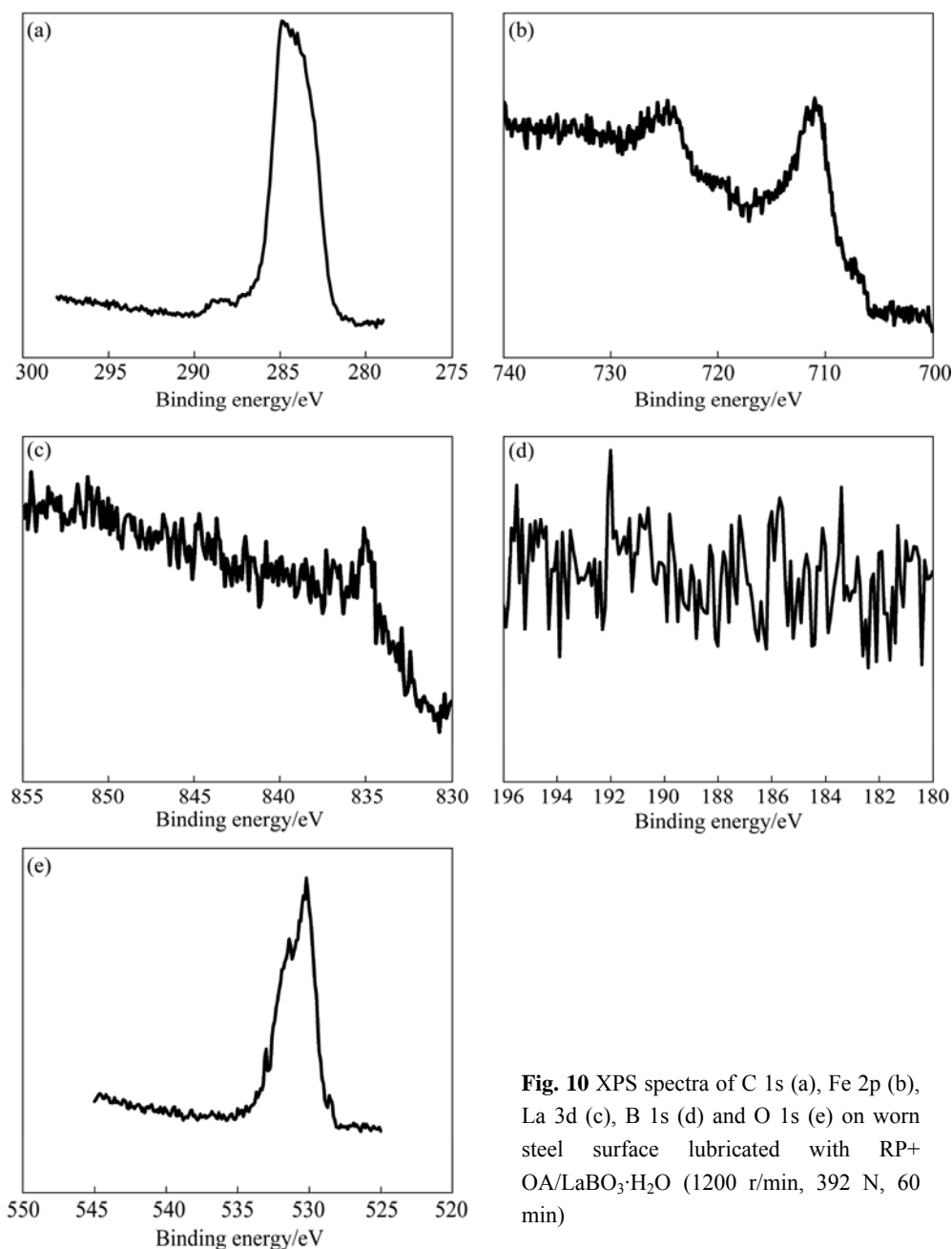


Fig. 10 XPS spectra of C 1s (a), Fe 2p (b), La 3d (c), B 1s (d) and O 1s (e) on worn steel surface lubricated with RP+OA/LaBO₃·H₂O (1200 r/min, 392 N, 60 min)

which is attributed to the adsorption or reaction of OA on the rubbed surfaces. The Fe 2p peak at 710.8 eV implies that iron is oxidized into Fe_2O_3 (Fig. 10(b)). The La 3d peak at 835.1 eV demonstrates that lanthanum exists on the rubbed surface in the chemical state of La_2O_3 (Fig. 10(c)). The B 1s peak at 192.0 eV indicates that B_2O_3 exists on worn steel surfaces (Fig. 10(d)). The O 1s peak at 531.4 eV reveals the existence of carbonyl groups, which is in good agreement with relevant IR analysis. At the same time, the O 1s peaks at 530.2, 533.0 and 528.6 eV correspond to the chemical state of oxygen in Fe_2O_3 , B_2O_3 and La_2O_3 , respectively (Fig. 10(e)).

According to the above-mentioned XPS analysis, it can be reasonably inferred that the friction-reducing and anti-wear mechanisms of OA/ $\text{LaBO}_3\cdot\text{H}_2\text{O}$ nanorods in RP are mainly ascribed to two aspects. On the one hand, OA can be physically and chemically adsorbed on sliding steel surfaces to form an adsorption film, thereby reducing friction and wear of the steel sliding pair. On the other hand, a complex boundary lubrication film mainly consisting of Fe_2O_3 , B_2O_3 and La_2O_3 forms on worn steel surfaces via tribochemical reaction, which is also contributed to an effective reduction of the wear and friction of the steel sliding pair.

4 Conclusions

1) Hydrophobic lanthanum borate nanorods were prepared by combining hydrothermal method with surface-modification by oleic acid. The as-prepared nanorods have an average diameter of 50 nm and a length of up to 500 nm.

2) Oleic acid plays an important role in the preparation process, which can obviously increase the aspect ratio of lanthanum borate nanorods.

3) The stoichiometry of lanthanum borate nanorods was determined, and the chemical composition was $\text{LaBO}_3\cdot\text{H}_2\text{O}$.

4) OA/ $\text{LaBO}_3\cdot\text{H}_2\text{O}$ nanorods can obviously improve the anti-wear and friction-reducing capacities of rapeseed oil. RP provides the optimal friction-reducing and anti-wear capacities at an OA/ $\text{LaBO}_3\cdot\text{H}_2\text{O}$ content of 1% (mass fraction). This is attributed to the formation of a complex boundary lubrication film which is mainly composed of the oxides of Fe_2O_3 , B_2O_3 and La_2O_3 as well as the formation of an adsorption film of OA on steel sliding surfaces.

References

[1] RYCENGA M, COBLEY C M, ZENG J, LI W Y, MORAN C H, ZHANG Q, QIN D, XIA Y N. Controlling the synthesis and assembly of silver nanostructures for plasmonic applications [J].

- Chemical Review, 2011, 111(6): 3669–3712.
- [2] ZHAO Li, LIU Zhi-hao, JIN Lei. Preparation and electrochemical performance of nano-scale $\text{Ni}(\text{OH})_2$ doped with zinc[J]. Transactions of Nonferrous Metals Society of China, 2013, 23(4): 392–399.
- [3] LI Jian-mei, CAI Chao, SONG Li-xiao, LI Jin-feng, ZHANG Zhao, XUE Min-zhao, LIU Yan-gang. Electrodeposition and characterization of nano-structured black nickel thin films [J]. Transactions of Nonferrous Metals Society of China, 2013, 23(8): 2300–2306.
- [4] KAO L H, HSU T C, LU H X. Sol-gel synthesis and morphological control of nanocrystalline TiO_2 via urea treatment [J]. Journal of Colloid Interface Science, 2007, 316(1): 160–167.
- [5] PARDO A, BUIJNSTERS J G, ENDRINO J L, GÓMEZ-ALEIXANDRE C, ABRASONIS G, BONET R, CARO J. Effect of the metal concentration on the structural, mechanical and tribological properties of self-organized α -C:Cu hard nanocomposite coatings [J]. Applied Surface Science, 2013, 280(1): 791–798.
- [6] YU He-long, XU Yi, SHI Pei-jing, XU Bin-shi, WANG Xiao-li, LIU Qian. Tribological properties and lubricating mechanisms of Cu nanoparticles in lubricant [J]. Transactions of Nonferrous Metals Society of China, 2008, 18(3): 636–641.
- [7] PENG D X, CHEN C H, KANG Y, CHANG Y P, CHANG S Y. Size effects of SiO_2 nanoparticles as oil additives on tribology of lubricant [J]. Industrial Lubrication and Tribology, 2010, 62(2): 111–120.
- [8] ZHANG Ling, CHEN Lei, WAN Hong-qi, CHEN Jian-min, ZHOU Hui-di. Synthesis and tribological properties of stearic acid-modified anatase (TiO_2) nanoparticles [J]. Tribol Letters, 2011, 41(2): 409–416.
- [9] YE Wen-yu, CHEN Tie-feng, YE Qing, GUO Xin-yong, ZHANG Zhi-jun, DANG Hong-xin. Preparation and tribological properties of tetrafluorobenzoic acid-modified TiO_2 nanoparticles as lubricant additives [J]. Materials Science and Engineering A, 2003, 359(1–2): 82–85.
- [10] WU Ji-fen, ZHAI Wen-sheng, JIE Gui-fen. Preparation and tribological properties of tungsten disulfide hollow spheres assisted by methyltriethylammonium chloride [J]. Tribology International, 2010, 43(9): 1650–1658.
- [11] HU K H, LIU M, WANG Q J, XU Y F, SCHRAUBE S, HU X G. Tribological properties of molybdenum disulfide nanosheets by monolayer restacking process as additive in liquid paraffin [J]. Tribology International, 2009, 42(1): 33–39.
- [12] ZHANG Jie, ZHANG Yu-juan, ZHANG Sheng-mao, YU Lai-gui, ZHANG Ping-yu, ZHANG Zhi-jun. Preparation of water-soluble lanthanum fluoride nanoparticles and evaluation of their tribological properties [J]. Tribol Letters, 2013, 52(2): 305–314.
- [13] HAN Bao-lei, LU Xin-chun. Effect of nano-sized CeF_3 on microstructure, mechanical and tribological properties of Ni–W composite coatings [J]. Surface and Coatings Technology, 2009, 203(23): 3656–3660.
- [14] ZHANG Ming, WANG Xiao-bo, LIU Wei-min. Tribological behavior of LaF_3 nanoparticles as additives in poly-alpha-olefin [J]. Industrial Lubrication and Tribology, 2013, 65(4): 226–235.
- [15] KONG Ling-tong, HU Hua, WANG Tian-you, HUANG Ding-hai, FU Jian-jian. Synthesis and surface modification of the nanoscale cerium borate as lubricant additive [J]. Journal of Rare Earths, 2011, 29(11): 1095–1099.
- [16] JIA Zheng-feng, XIA Yan-qiu. Hydrothermal synthesis, characterization, and tribological behavior of oleic acid-capped lanthanum borate with different morphologies [J]. Tribol Letters, 2011, 41(2): 425–434.
- [17] SUN Lei, ZHOU Jing-fang, ZHANG Zhi-jun, DANG Hong-xin. Synthesis and tribological behavior of surface modified $(\text{NH}_4)_3\text{PMo}_{12}\text{O}_{40}$ nanoparticles [J]. Wear, 2004, 256(1–2): 176–181.

- [18] YE Yi, DONG Jun-xiu, CHEN Bo-shui, HU Ze-shan, FAN Jin-fu, YE Xue-jun. Effect of wear resistance on nanometer lanthanum borate in lubricating oils [J]. *Lubrication Engineering*, 2000(2): 22–24. (in Chinese)
- [19] CHEN Bo-shui, FANG Jian-hua, WANG Jiu, LI Jia, LOU Fang. Friction and wear performance of borates and lanthanum chloride in water [J]. *Journal of Rare Earths*, 2008, 26(4): 590–593.
- [20] HU Z S, DONG J X, CHEN G X, HE J Z. Preparation and tribological properties of nanoparticles lanthanum borate [J]. *Wear*, 2000, 243(1–2): 43–47.
- [21] MOSLEH M, ATNAFU N D, BELK J H, NOBLES O M. Modification of sheet metal forming fluids with dispersed nanoparticles for improved lubrication [J]. *Wear*, 2009, 267(5): 1220–1225.
- [22] LIU Ning, TIAN Yu-mei, YU Lian-xiang, LI Quan-jun, MENG Fan-yu, ZHENG Yun-hui, ZHANG Guang-yu, LIU Zhi-hui, LI Jing, JIANG Fu-ming. Synthesis and surface modification of uniform barium borate nanorods for lubrication [J]. *Journal of Alloys and Compounds*, 2008, 466(1–2): L11–L14.
- [23] BAO Shu-juan, BAO Qiao-liang, LI Chang-ming, CHEN Tu-pei, SUN Chang-qing, DONG Zhi-li, GAN Ye, ZHANG Jun. Synthesis and electrical transport of novel channel-structured β -AgVO₃ [J]. *Small*, 2007, 3(7): 1174–1177.
- [24] SINGH D P, POLYCHRONOPOULOU K, REBHOLZ C, AOUADI S M. Room temperature synthesis and high temperature frictional study of silver vanadate nanorods [J]. *Nanotechnology*, 2010, 21(32): 325601–325607.
- [25] LIN Jing, HUANG Yang, ZHANG Jun, DING Xiao-xiao, QI Shou-ren, TANG Cheng-cun. Preparation and characterization of lanthanum borate nanowires [J]. *Materials Letters*, 2007, 61(7): 1596–1600.
- [26] HAO Li-feng, LI Jiu-sheng, XU Xiao-hong, REN Tian-hui. Preparation and tribological properties of a kind of lubricant containing calcium borate nanoparticles as additives [J]. *Industrial Lubrication and Tribology*, 2012, 64(1): 16–22.
- [27] LEMANCEAU S, BERTRAND-CHADEYRON G, MAHIOU R, EI-GHOZZI M, COUSSEINS J C, CONFLANT P, VANNIER R N. Synthesis and characterization of H LnBO₃ orthoborates (Ln=La, Nd, Sm, and Eu) [J]. *Journal of Solid State Chemistry*, 1999, 148(2): 229–235.
- [28] TIAN Yu-mei, GUO Yu-peng, JIANG Man, SHENG Ye, HARI B, ZHANG Guang-yu, JIANG Yan-qiu, ZHOU Bing, ZHU Yan-chao, WANG Zi-chen. Synthesis of hydrophobic zinc borate nanodiscs for lubrication [J]. *Materials Letters*, 2006, 60(20): 2511–2515.
- [29] QIAN Jian-hua, YIN Xiang-yu, WANG Ning, LIU Lin, XING Jin-juan. Preparation and tribological properties of stearic acid-modified hierarchical anatase TiO₂ microcrystals [J]. *Applied Surface Science*, 2012, 258(7): 2778–2782.

疏水性硼酸镧纳米棒的制备及其在菜籽油中的摩擦磨损性能

谷科城¹, 陈波水¹, 王雪梅², 王九¹, 方建华¹, 吴江¹, 黄立川³

1. 后勤工程学院 油料应用与管理工程系, 重庆 401311;

2. 后勤工程学院 化学与材料工程系, 重庆 401311;

3. 成都军区 物资油料部, 成都 610015

摘要: 采用水热法合成油酸修饰的硼酸镧纳米棒(OA/LaBO₃·H₂O), 利用 X 射线衍射和扫描电镜等测试技术对其微观结构进行表征, 并在四球摩擦试验机上考察其在菜籽油中的摩擦磨损性能。结果表明, 所制备的 OA/LaBO₃·H₂O 为直径约 50 nm、长达 500 nm 的疏水性纳米棒。OA/LaBO₃·H₂O 能显著提高菜籽油的抗磨减摩性能; 当 OA/LaBO₃·H₂O 的添加量为 1%(质量分数)时, 菜籽油的抗磨减摩性能最佳。

关键词: 硼酸镧; 纳米棒; 疏水性; 制备; 摩擦; 磨损; 菜籽油

(Edited by Wei-ping CHEN)